Energy & Environmental Science

ROYAL SOCIETY OF CHEMISTRY

PAPER

View Article Online
View Journal | View Issue

Cite this: *Energy Environ. Sci.*, 2024, **17**, 183

HCO_3^--mediated highly efficient photoelectrochemical dioxygenation of arylalkenes: triple roles of HCO_3^--derived radicals†

Jie Yang,[ab] Yukun Zhao,[ab] Mengyu Duan,[ab] Chaoyuan Deng,[ab] Yufan Zhang,[ab] Yu Lei,[ab] Jikun Li,[ab] Wenjing Song,[ab] Chuncheng Chen *[ab] and Jincai Zhao[ab]

Received 4th September 2023,
Accepted 9th November 2023

DOI: 10.1039/d3ee02948d

rsc.li/ees

Alkene dioxygenation reactions are significant organic transformation process, but the direct oxidation of alkenes on photoanodes exhibits quite poor yields for dioxygenation products. Here, we report that the presence of bicarbonate in a heterogenous photoelectrochemical (PEC) cell can achieve efficient dioxygenation of alkenes under mild conditions. A broad range of alkene substrates with a variety of substitute groups can be effectively oxygenated to diols or α-hydroxy ketones, with a product yield of up to 89%. Furthermore, we identified that the diol product is formed *via* a peroxydiol intermediate. Spin-trap electron paramagnetic resonance (EPR) experiments show that the HCO_3^--derived radicals are important active species. Accordingly, we propose a triple role for formed HCO_3^--derived radicals in the dioxygenation of alkenes: attacking the C=C bond of the alkene to initiate the reaction, producing $^{\bullet}CO_4^-$ active species for the formation of a peroxydiol intermediate, and reducing the peroxydiol to a diol. The present work provides a promising strategy for the transformation of alkenes with green radicals and paves the way for the application of HCO_3^- in PEC organic synthesis.

Broader context

Solar-driven photoelectrochemical (PEC) processes, including the splitting of water, CO_2 reduction and pollutant degradation, represent sustainable methods for harnessing solar energy. Among these, water splitting for hydrogen production is the most extensively investigated. However, the kinetics of the oxygen evolution reaction are inherently unfavorable, and the resulting O_2 holds minimal economic value. Thus, it is imperative to explore alternative reactions that yield high-value fine chemicals at the photoanode. The oxidation of alkenes has garnered significant attention, given the critical role of their products, such as diols and epoxides, as essential intermediates in numerous valuable chemical processes. PEC alkene oxidation has emerged as a sustainable and secure pathway to achieve this objective, while concurrently enhancing the rate of hydrogen production at the cathode. Nevertheless, the direct selective oxidation of alkenes on the photoanode surface poses formidable challenges. This study presents an innovative HCO_3^--mediated PEC system, leveraging diverse reaction pathways facilitated by HCO_3^--derived radicals, to achieve the highly selective dioxygenation of olefin coupled with the hydrogen evolution reaction. The triple roles of HCO_3^--derived radicals were identified experimentally for selective dioxygenation. We believe that our research provides a promising strategy for the transformation of alkenes with "green" radicals, and paves the way for the application of HCO_3^- in PEC synthesis.

Introduction

Photoelectrochemistry[1] represents a sustainable method for solar energy conversion by driving reactions such as water splitting,[2,3] CO_2 reduction[4] and pollutant degradation.[5,6] PEC water splitting for hydrogen production is the most widely studied PEC process. In this reaction, the water molecule is oxidized to generate O_2 (oxygen evolution reaction, OER) at the photoanode, while the released proton is reduced to produce hydrogen (hydrogen evolution reaction, HER) on the cathode. The OER is kinetically unfavourable, and the formed dioxygen has little economic value. It is also feasible to explore alternative reactions that produce high-value fine chemicals instead of dioxygen on the photoanode. For example, the oxidation of organic substrates or the mediated oxidation of organic substrates not only increases the rate of cathode hydrogen evolution,[7,8] but also produces high value-added chemicals, exhibiting a higher economic benefit than that of water oxidation.

[a] *Key Laboratory of Photochemistry, Beijing National Laboratory for Molecular Sciences, Institute of Chemistry Chinese Academy of Sciences, Beijing 100190, P. R. China. E-mail: ccchen@iccas.ac.cn*

[b] *University of the Chinese Academy of Sciences, Beijing 100049, P. R. China*

† Electronic supplementary information (ESI) available. See DOI: https://doi.org/10.1039/d3ee02948d

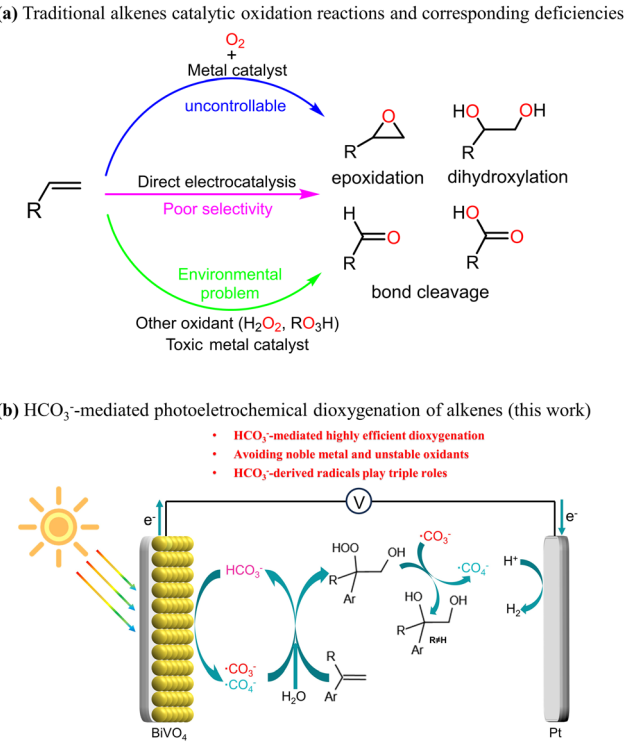

Scheme 1 Comparison of the different pathways for the oxidation of alkenes.

The oxidation of olefins is one of the most important methods for converting mineral oil into high value-added chemicals[9,10] (Scheme 1). In recent years, there has been significant attention on the electrochemical (EC) or PEC oxidation of olefins coupled with the HER, in which the requirement for external harsh oxidants can be avoided. However, achieving the direct selective oxidation of olefins at photoanodes towards selectivity of a given product is challenging.[11] This difficulty is likely attributed to the large steric hindrance and low polarity of C=C double bonds, making it unfavourable for the olefins to interact efficiently with the surface of the photoanode.[12] Utilizing redox mediators, indirect EC or PEC oxidations have been reported to markedly promote the selective performance of high-value products.[13,14] For instance, Sargent's group reported the chloride-mediated EC epoxidation of ethylene and propylene with 97% selectivity and 71% Faraday efficiency (FE).[13] Recent research conducted by our team and Li's team revealed the bromine-mediated PEC epoxidation of olefins on α-Fe_2O_3[12] and $BiVO_4$,[8] respectively, which both demonstrated good selectivity, while they exhibited extremely poor PEC epoxidation performance in the absence of bromine.

In recent years, HCO_3^- has been utilized as an EC or PEC mediator for producing hydrogen peroxide[15–18] and degrading contaminants.[19,20] For example, it has been reported that carbonate-mediated EC water oxidation shows high selectivity for H_2O_2 production through the formation of carbonate radical and percarbonate intermediates.[18] The PEC degradation rate of rhodamine B (a pollutant model) with HCO_3^- as an electrolyte was found to be 30% higher than that using SO_4^{2-} as a electrolyte,[19] which is attributed to the mediating effect of the carbonate radical. It is worth noting that the redox potential of $^{\bullet}CO_3^-/HCO_3^-$ is relatively low (E_0 = 1.78 V, pH = 7).[21] In various hydroxyl radical-based advanced oxidation processes, HCO_3^- has been found to transform the photoinduced hole or hydroxyl free radical to the less active carbonate radical, and thus significantly inhibit the degradation of organic pollutants.[22] Although the mild oxidation capacity of the carbonate radical is unfavourable for the degradation of organic pollutants, it provides a significant advantage in selectively oxidizing substrates with certain functionality by avoiding overoxidation or mineralization. Therefore, theoretically, HCO_3^- should be ideal for selective oxidation in EC or PEC reactions. However, the application of HCO_3^--mediated oxidation reactions in organic synthesis has rarely been reported to date.

In this study, we present HCO_3^- as an excellent redox mediator for the highly-selective PEC dioxygenation of alkenes, in which these dioxygenation products have been applied in organic synthesis[23–25] and pharmaceuticals.[26,27] HCO_3^--mediated dioxygenation reactions can effectively address these challenges suffered in other systems, including toxic noble metal catalysts, the requirement for external oxidants and the incompatibility between the hydrophilicity of the photoanode surface and the hydrophobicity of the C=C bond, which arises mainly because the hydrophilic HCO_3^- is easily oxidized to $^{\bullet}CO_3^-$ on the $BiVO_4$ surface, and the $^{\bullet}CO_3^-$ can diffuse into the bulk solution and react with the organic substrate.[28,29] Moreover, the protocol demonstrates excellent functional group tolerance. Mechanistic studies further verify that HCO_3^--derived radicals play triple roles in the alkene dioxygenation reaction.

Results and discussion

HCO_3^--mediated arylalkene dioxygenation reactions

All PEC reactions were conducted in an undivided cell with a three-electrode configuration (unless otherwise stated). $BiVO_4$ was first employed as the photoanode, with Pt wire and Ag/AgCl serving as the counter electrode and reference electrode, respectively. The PEC performance of synthetic $BiVO_4$ was tested in 0.5 M potassium borate buffer (KBi) solution with a pH of 9.5, and the addition of CH_3CN was found to not affect the photocurrent of $BiVO_4$ under the same applied potential (Fig. S2, ESI†). 4-Chloro-alpha-methylstryene (**4aa**) was chosen as the model substrate to explore the reaction conditions (Table 1). The reaction was conducted in a solution mixture of H_2O and CH_3CN (volumetric ratio of 1 : 1) with $KHCO_3$ as the electrolyte. Under these conditions, after 1.5 h of reaction at an applied potential of 0.8 V (potentials given in this study are referenced to the Ag/AgCl electrode unless otherwise stated), approximately 95% of **4aa** was converted, and the selectivity of the diol product (**4a**) reached around 89%, with a yield of 85% (Table 1, entry 1) and a FE of 15%. The low FE may be caused by the formation of by-products (Fig. S3a, ESI†), and the hydrolysis of HCO_4^- to H_2O_2 (Fig. S3b, ESI†) and further to O_2. As the reaction progresses, the substrate is gradually consumed,

Table 1 The photoelectrochemical dioxygenation of **4aa** under different conditions

Entry	Reaction conditions[a]	Selectivity (%)	Yield[b] (%)
1	50% H_2O	89 ± 2	85 ± 3 (80)[c]
2	Without light	n.d.[d]	n.d.[d]
3	Without applied potential	n.d.[d]	n.d.[d]
4	1.4 V	91 ± 1	64 ± 2
5	0.2 V[e]	72 ± 2	71 ± 2
6	$NaHCO_3$	82 ± 3	75 ± 3
7	NH_4HCO_3	88 ± 1	79 ± 3
8	Ar atmosphere	87 ± 1	81 ± 1
9	TiO_2	81 ± 2	78 ± 1
10	α-Fe_2O_3	Trace[f]	Trace

[a] Reaction conditions: $BiVO_4$ photoanode (2.5 cm^2), Pt cathode, an Ag/AgCl electrode (3.5 M KCl leak-free and 2.0 mm diameter) was used as the reference electrode, CH_3CN/H_2O (v : v = 1 : 1, 5 mL), under AM 1.5G illumination, 0.1 M $KHCO_3$ was used as the electrolyte. The initial concentration of the substrate was 4 mM, the applied potential was 0.8 V *versus* Ag/AgCl, under an air atmosphere, room temperature, and the time of the reaction was 1.5 h, undivided cell. [b] The quantity of the products determined by ^1H NMR using 1,3,5-trimethoxybenzene as an internal standard and substrates were analyzed and quantified using an Agilent HPLC1260 system. [c] Isolated yield. [d] Not detected. [e] The reaction time was 3 h. [f] Trace product was detected.

resulting in a corresponding increase in the diol product (Fig. S4a, ESI†), and the selectivity of the product remains almost unchanged (Fig. 1(a)). In addition, the FE of the product gradually decreases with an increase in the reaction time. This phenomenon may be attributed to the substrate concentration also decreasing with an increase in the reaction time, so the probability of the collision between the substrate and the carbonate active species also decreases, resulting in a decrease in the FE of the product. However, no product was detected in the absence of light or applied potential (Table 1, entries 2 and 3). When the applied potential exceeds 0.8 V, the selectivity of **4a** is well maintained (Table S1, ESI† entry 16 and Table 1, entry 4), while the conversion significantly decreases over the same photoelectrolysis time due to the competition of the OER at a higher potential. At a lower applied potential (Table 1, entry 5 and Table S1, ESI† entries 14 and 15), a decrease in selectivity is observed, which may be assigned to the poor separation

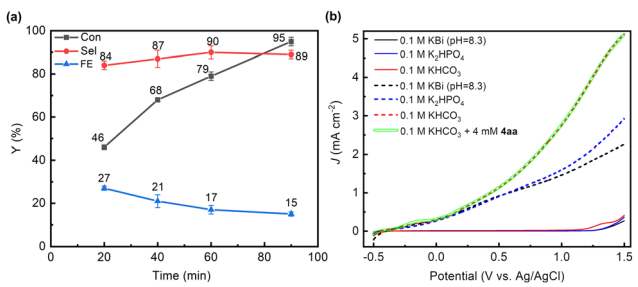

Fig. 1 (a) Time-dependent conversion (Con) of 4.0 mM **4aa**, selectivity (Sel) and Faraday efficiency (FE) of the product (**4a**) with 0.1 M $KHCO_3$ solution (CH_3CN/H_2O = 1 : 1) under an air atmosphere at 0.8 V *vs.* Ag/AgCl on $BiVO_4$ under AM 1.5G illumination. (b) LSV curves of $BiVO_4$ under AM 1.5G illumination (dashed and green lines) and in the dark (solid lines) measured in 0.1 M $KHCO_3$, 0.1 M KBi (potassium borate buffer (pH = 8.3)) or 0.1 M K_2HPO_4 solution (CH_3CN/H_2O = 1 : 1) on $BiVO_4$.

efficiency of photogenerated carriers, leading to inadequate charge accumulation. The FE of H_2 produced at the cathode reaches approximately 95% (Fig. S5, ESI†), indicating that the cathodic reaction predominantly involves a water reduction reaction.

Replacing $KHCO_3$ with equivalent amounts of K_2HPO_4, KBi (potassium borate buffer (pH = 8.3)), KAc (potassium acetate) and KNO_3 completely suppresses the alkene dioxygenation process, in which the substrate is barely consumed (Fig. S6, ESI†). When Cl^- that is able to be oxidized is used, alkenes can be converted but there is little dioxide product. These experimental results indicate that HCO_3^- plays a key role in mediating the dioxygenation process of alkenes. Moreover, when the cation K^+ of $KHCO_3$ is replaced by Na^+ or NH_4^+ (Table 1, entries 6 and 7), high yields of the diol product are still observed. These experimental results strongly indicate that HCO_3^- plays a pivotal role in alkene dioxygenation reactions. We investigated the influence of electrolyte acidity/basicity by adjusting the pH of the water with KOH or CO_2 gas. As shown in Table S1 (ESI†), the yields of the diol product remain almost unchanged (about 85%) when water with a pH range of 6.8–9.3 is used (Table S1, ESI† entries 1–3). A further increase in pH reduces the yield of diol (Table S1, ESI† entries 4 and 5). Considering the pK_{a_1} (6.37) and pK_{a_2} (10.32) of H_2CO_3, the high yield of diol in the pH range of 6.8–9.3 suggests that HCO_3^- is the dominant active species in mediating the alkene dioxygenation reaction. Furthermore, we carried out the reaction in an H-type cell with a proton exchange membrane (Fig. S7a, ESI†) and found that the HCO_3^--mediated PEC alkene dioxygenation reaction only occurs at the photoanode (Fig. S7b, ESI†). When the reaction is carried out under an Ar atmosphere (Table 1, entry 8), similar selectivity and yield for the dioxygenation are observed compared to those in air, indicating that O_2 is not involved in the alkene dioxygenation pathway.

The dioxygenation reaction can also occur on TiO_2 photoanodes, although the yield is somewhat lower than that on $BiVO_4$ (Table 1, entry 9), which is due to the strong oxidation capacity of TiO_2 leading to an increase in by-products (Fig. S8b, ESI†). When the α-Fe_2O_3 is employed as the photoanode, negligible substrate reactivity is observed (Fig. S8c, ESI†). Moreover, the photocurrent of α-Fe_2O_3 photoanode shows little change when HCO_3^- is added to the solution (Fig. S9, ESI†). This phenomenon is attributed to the insufficient oxidation capacity of α-Fe_2O_3, making it difficult to oxidize HCO_3^- to $^\bullet CO_3^-$ and consequently hinders the conversion of alkenes.

Scope of substrates

With the optimized protocol for alkene dioxygenation reactions in hand, the scope of the bicarbonate-mediated photoelectrochemical dioxygenation of alkenes was explored (Table 2). Initially, various monofunctionalized α-methyl-styrene substrates with *para*-, *meta*- or *ortho*-substituents were dioxygenated to the corresponding products in good yields. Notably, the substrates with electron-withdrawing groups can be efficiently converted to the corresponding diols smoothly (**1a–5a**), while the strong electron-donating groups (such as –OCH_3 (**6a**),

Table 2 Scope of the substituted aryl alkenes for the PEC HCO_3^--mediated alkene dioxidation

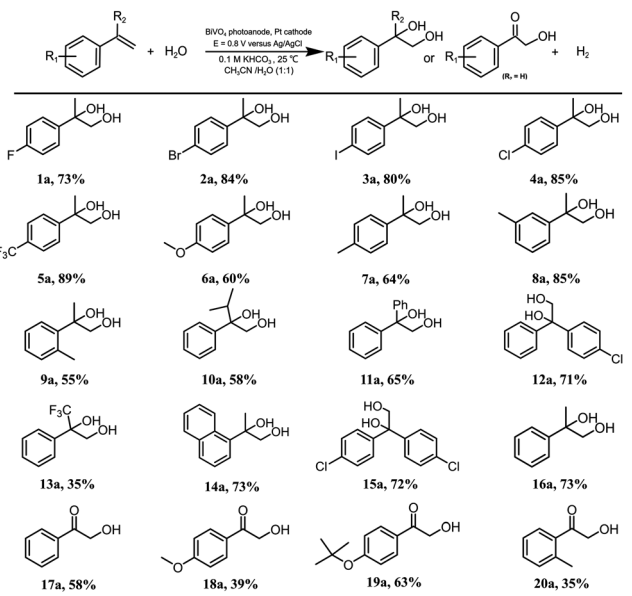

Reaction conditions: $BiVO_4$ photoanode (2.5 cm^2), Pt cathode, an Ag/AgCl electrode (3.5 M KCl leak-free and 2.0 mm diameter) was used as the reference electrode, CH_3CN/H_2O (2.5/2.5 mL), under AM 1.5G illumination, 0.1 M $KHCO_3$ was used as the electrolyte and the initial concentration of the substrate was 4.0 mM, in air, room temperature, photoelectrolysis reaction time of 1.5-3 h. Quantity of products determined by ^1H NMR using 1,3,5-trimethoxybenzene as internal standard and substrates were analyzed and quantified by using an Agilent HPLC1260 system.

$-CH_3$ (**7a**)) show a slight decrease in the yields of their products. The diol yield of the *meta*-methyl-substituted α-methyl-styrene (**8a**) is significantly higher than those of the *para*- and *ortho*-substituted substrates (**7a**, **9a**), confirming that the substituent effect is important to the dioxygenation. In addition, when the α position of styrene is substituted by isopropyl (**10a**), phenyl (**11a**), 4-chlorobenzene (**12a**) or trifluoromethyl (**13a**), the corresponding products are obtained in good yields. Moreover, substrates with polycyclic rings, such as naphthalene (**14a**), also yield the dioxygenation product with good efficiency.

Various substituents of styrene derivatives without an α-substitutent could be oxidized to the corresponding α-hydroxy ketones under the aforementioned reaction conditions (**17a–20a**). The formation of α-hydroxy ketones may originate from the highly active hydrogen atom in the α-position, which undergoes further oxidation. In contrast, α-methyl styrene, which has a methyl group occupied at the α-position, could not be further oxidized, so the diol product remained. Generally, the selectivity and yield for α-hydroxy ketone formation during styrene oxidation are significantly lower than those of α-methyl-styrenes, which may be caused by further oxidation involving C–C bond breakage during the process of forming α-hydroxy ketone products. To assess the stability of the substrates under light exposure, several characteristic substrates were selected for stability testing experiments. As shown in Fig. S11 (ESI†), the concentration of these substrates remained unchanged over 2 h of light exposure, affirming that all organic substrates were stable under illumination.

For gram-scale synthesis, 4-chloro-alpha-methyl-stryene was chosen as a substrate to conduct the dioxygenation reaction. We chose a substrate concentration of 20 mM for gram-scale synthesis, which has a higher FE (Fig. S12, ESI†). The reaction solution volume was increased by thirty times (Fig. S13, ESI†) compared to that of the standard condition. 0.44 gram of diol product **4a** with an 80% yield was obtained and the selectivity and FE were 90% and 52%, respectively. This higher FE may be caused by the increase in the substrate concentration, which improves the probability of interaction between the substrate and active species. For the stability of the $BiVO_4$, PEC tests and characterization were conducted. As depicted in Fig. S14a and b (ESI†), the PEC behavior remained almost unchanged after 6 h of photoelectrolysis. XRD patterns (Fig. S14c, ESI†), UV-vis adsorption spectra (Fig. S14d, ESI†), surface components (XPS) (Fig. S15, ESI†) and SEM (Fig. S16, ESI†) of the $BiVO_4$ photoanode before and after photoelectrolysis also revealed that the properties and morphology of the photoanodes showed no obvious changes. These results demonstrate that $BiVO_4$ exhibits superior stability under standard reaction conditions.

Alkene dioxygenation mechanism

In order to gain more insight into the alkene dioxygenation reaction, linear sweep voltammetry (LSV) tests were performed under different conditions. Compared to using K_2HPO_4 and KBi as the electrolyte, a noticeable enhancement in photocurrent was observed in the $KHCO_3$ system when the applied potential exceeded 0.2 V (Fig. 1(b)), indicating that the oxidation of HCO_3^- occurs prior to water oxidation. Although the oxidation of water to oxygen (E_{O_2/H_2O} = 1.23 V *vs.* RHE) is more thermodynamically advantageous than the oxidation of HCO_3^- ($E_{\bullet CO_3^-/HCO_3^-}$ = 1.78 V *vs.* RHE), HCO_3^- is oxidized to $^\bullet CO_3^-$ *via* a single-electron-transfer pathway and water is oxidized to oxygen *via* a four-electron process, which is characterized by unfavorable kinetics. Therefore, the oxidation of HCO_3^- is superior to that of water, which has been reported in previous reports.[17,18] Furthermore, the photocurrent exhibits negligible variation upon the addition of **4aa** in the HCO_3^- system, suggesting that the direct oxidation of alkenes on the photoanode occurs at a neglectable rate. The redox potential of $^\bullet CO_3^-/HCO_3^-$ *via* a single electron oxidation (eqn (1)) is 1.78 V *vs.* NHE.[21] Notably, the valence band potential of $BiVO_4$ registers at 2.4 V,[30] surpassing the redox potential of $^\bullet CO_3^-/HCO_3^-$. Consequently, $BiVO_4$ effectively promotes the oxidation of HCO_3^-, leading to formation of $^\bullet CO_3^-$. These experimental and theoretical data indicate that the alkene dioxygenation reaction may be mediated by generated carbonated active species. To validate this proposition, 2,2,6,6-tetramethyl-1-piperidinyloxy (TEMPO, 3 equiv.) or 2,6-di-*tert*-butyl-4-methylphenol (BHT, 3 equiv.), which are typical radical scavengers for trapping reactive radicals,[31] were added into the reaction system. Strikingly, the presence of radical scavengers resulted in nearly complete inhibition of alkene dioxygenation (Table 3, entries 2 and 3),

Table 3 Mechanism exploration with the controlled experiments

Entry	Reaction conditions[a]	Selectivity (%)	Yield (%)
1	0.1 M $KHCO_3$	89 ± 2	85 ± 3
2	3 equiv. TEMPO[c]	Trace[b]	Trace[b]
3	3 equiv. BHT[d]	Trace[b]	Trace[b]
4	Add 1 mM H_2O_2	80 ± 1	76 ± 1
5	Add 1 M H_2O_2	n.d.[e]	n.d.[e]
6	Add 1 M H_2O_2, no PEC	n.d.[e]	n.d.[e]
7	3 equiv. *t*-BuOH[f]	86 ± 3	82 ± 2

[a] Standard reaction conditions: $BiVO_4$ photoanode (2.5 cm^2), Pt cathode, CH_3CN/H_2O (2.5/2.5 mL), under AM 1.5G illumination, 0.1 M $KHCO_3$ was used as the electrolyte and the initial concentration of the substrate was 4.0 mM, under air, room temperature, reaction time of 1.5 h, undivided cell. [b] Trace alkene dioxygenation product was detected. [c] 2,2,6,6-Tetramethyl-1-piperidinyloxy (TEMPO). [d] 2,6-Di-*tert*-butyl-4-methylphenol (BHT). [e] Not detected. [f] *tert*-butanol (*t*-BuOH).

implying the involvement of active radical species in the dioxygenation process.

$$HCO_3^- \rightarrow {}^\bullet CO_3^- + H^+ + e^- \quad (1)$$

$$HCO_3^- + H_2O \rightarrow HCO_4^- + 2H^+ + 2e^- \quad (2)$$

$$HCO_4^- + H_2O \rightarrow HCO_3^- + H_2O_2 \quad (3)$$

It has been reported that HCO_3^- can be oxidized to ${}^\bullet CO_3^-$ (eqn (1)) through single electron oxidation,[18] or to HCO_4^- *via* a two-electron process (eqn (2))[17,32] and HCO_4^- can be hydrolyzed to hydrogen peroxide (eqn (3))[33] in the EC or PEC processes. Based on previous research, there are potential active species, ${}^\bullet CO_3^-$, H_2O_2 and HCO_4^-, which are capable of initiating the reaction. To elucidate the contributions of H_2O_2 and HCO_4^-, controlled experiments were conducted. Firstly, the addition of H_2O_2 triggered a slight decrease of dioxygenation activity (Table 3, entry 4), excluding the possibility that H_2O_2 (if formed) acts as the active species of dioxygenation. With an increase in the H_2O_2 concentration, the dioxygenation reaction is even suppressed (Table 3, entry 5), which might be attributed to the competitive oxidation caused by H_2O_2. Subsequently, to assess the role of HCO_4^-, the HCO_4^- species were *in situ* produced by a mixing reaction of abundant H_2O_2 and HCO_3^- (without an applied potential).[34] No reaction was detected under these conditions (Table 3, entry 6), ruling out the participation of HCO_4- species. Moreover, the addition of *tert*-butanol, a typical ${}^\bullet OH$ scavenger,[35] showed negligible effects on the selectivity and yield of the diol product (Table 3, entry 7), indicating that ${}^\bullet OH$ is not the active species of dioxygenation. Consequently, it is reasonable to infer that ${}^\bullet CO_3^-$ serves as the primary active species in the dioxygenation process.

Considering the difference in products obtained from styrene and alpha-methyl-styrene, it is plausible that the formation of α-hydroxyacetophenone through the oxidation of styrene proceeds *via* a diol-intermediate pathway, where a diol is initially formed and subsequently dehydrogenated to produce the α-hydroxy ketone. However, when the diol was directly employed as the substrate, the selectivity and yield of the α-hydroxyacetophenone product were only 64% and 35%, respectively. These values were lower than the selectivity (78%) and yield (57%) achieved with styrene as the substrate under the same reaction conditions (Table S2, ESI† entries 1 and 2). Thus, it is evident that the diol does not act as the intermediate for the formation of α-hydroxy ketone.

In addition, acetophenone and styrene epoxide were employed as substrates and a slight reaction was observed (Table S2, ESI† entries 3 and 4), suggesting that ketone and epoxide are also not the intermediates. Interestingly, when peroxydiol (**4ab**) was used as the substrate, excellent diol product selectivity (96%) and yield (95%) were obtained within 1 h of the PEC reaction (Fig. 2(b) and (d)), indicative that peroxydiol may be a true reaction intermediate in the dioxygenation process. This peroxydiol intermediate was also detected during the PEC oxidation of **4aa** on $BiVO_4$, and the concentration of the intermediate **4ab** showed an initial increase followed by a subsequent decrease with an increase in the reaction time (Fig. 2(c)). It has been reported that the transformation from peroxydiol to diol is a two-electron reduction process, typically requiring a reductant such as triphenylphosphine (PPh_3).[36,37] To make clear whether the reduction of peroxydiol occurs on the anode or cathode, the reaction was carried out in an H-type cell. The results demonstrate that the reduction reaction from peroxydiol to diol occurs in the photoanode compartment (Fig. S17, ESI†). However, no reduction reaction was observed in the absence of HCO_3^-, irradiation or applied potential (Table S3, ESI†), highlighting the crucial role of ${}^\bullet CO_3^-$ in facilitating the reductive reaction. These observations further imply that the formation of diol originates from the interaction between ${}^\bullet CO_3^-$ and peroxydiol. Stoichiometrically, the attack of the peroxy group of the peroxydiol by ${}^\bullet CO_3^-$ led to the formation of a ${}^\bullet CO_4^-$ radical and diol product, which may be analogous to the reaction between HCO_3^- and H_2O_2 to form HCO_4^- and H_2O, as reported in the previous literature.[38]

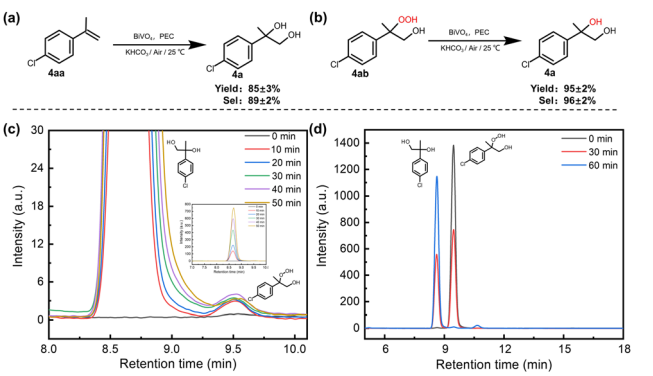

Fig. 2 (a) and (b) Experiments of different substrate reactions under standard conditions. (c) The HPLC spectra obtained different photoelectrolysis time of 4.0 mM **4aa** with 0.1 M $KHCO_3$ at 0.8 V *vs.* Ag/AgCl on $BiVO_4$ (illustration is the corresponding full-size image). (d) The HPLC spectra obtained different photoelectrolysis time of 4.0 mM peroxydiol (**4ab**) with 0.1 mM $KHCO_3$ at 0.8 V *vs.* Ag/AgCl on $BiVO_4$. Quantity of products determined by ^1H NMR using 1,3,5-trimethoxybenzene as an internal standard and substrates were analyzed and quantified using an Agilent HPLC1260 system.

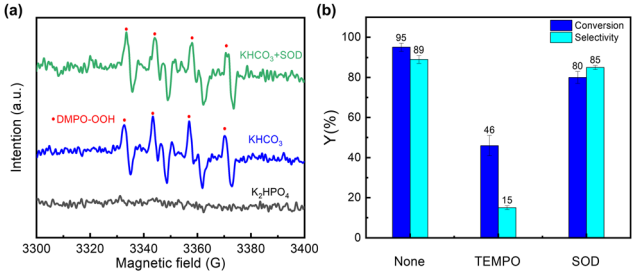

Fig. 3 (a) EPR spectra of DMPO adducts in different systems. (b) Effects of different scavengers on the reaction activity.

To examine the formation of radical species, 5,5-dimethyl-1-pyrroline N-oxide (DMPO) was used as a spin-trapping reagent for conducting EPR experiments. As shown in Fig. 3(a), a signal corresponding to peroxyradical species (DMPO-OOH) was detected in the presence of HCO_3^-, whereas no signal was observed when HCO_3^- was replaced by K_2HPO_4. The results suggest that HCO_3^- is involved in the formation of the superoxide adduct of DMPO. This DMPO-OOH signal remains unaltered upon adding superoxide dismutase (SOD) (0.2 mg ml^{-1}) (Fig. 3(a)), meaning that this adduct is not formed from the trapping of the superoxide radical by DMPO. Therefore, a distinct radical species, rather than superoxide radicals, is responsible for the formation of the DMPO-OOH adduct. It has been reported that the interaction of $^{\bullet}CO_3^-$ and HCO_4^- can yield $^{\bullet}CO_4^-$.[39] Therefore, it is reasonable to propose that DMPO may trap $^{\bullet}CO_4^-$ to form a DMPO-CO_4^- adduct, which is rapidly hydrolyzed to DMPO-OOH and HCO_3^- (Fig. S18b, ESI†). This is why the dioxygenation activity is well maintained upon the addition of SOD (Fig. 3(b)). Thus, it is highly plausible that $^{\bullet}CO_4^-$ acts as the key active species to further trigger dioxygenation reaction. In addition, by conducting EPR experiments under different applied potentials (Fig. S19, ESI†), it is obvious that the signal of DMPO-OOH is significantly decreased when the applied potential is reduced. This indicates that the generation of $^{\bullet}CO_4^-$ is indeed reduced at low potential, leading to a decrease in the product selectivity.

As shown in Scheme 2, the first step for PEC alkene dioxygenation is the oxidation of HCO_3^- to generate $^{\bullet}CO_3^-$ and $^{\bullet}CO_4^-$ species, which could be obtained by direct oxidation or a $^{\bullet}CO_3^-$-mediated process on the photoanode (step 1). Then, $^{\bullet}CO_3^-$ further attacks the terminal C atom of the C=C bond of the alkene ($\mathbf{a_1}$), leading to the formation of a carbonated radical ($\mathbf{a_2}$). This carbonated radical undergoes rapid hydrolysis to generate a hydroxylated carbon radical ($\mathbf{a_3}$). Subsequently, the generated carbon radical combines with $^{\bullet}CO_4^-$ to form a peroxycarbonated intermediate, which ultimately undergoes hydrolysis to a peroxydiol ($\mathbf{a_4}$). Finally, the peroxydiol is reduced to a diol ($\mathbf{a_6}$) by $^{\bullet}CO_3^-$, with the simultaneous regeneration of $^{\bullet}CO_4^-$ (step 5). Conversely, if styrene is employed as the substrate, the peroxydiol rapidly dehydrates to form an α-hydroxy ketone product ($\mathbf{a_5}$). According to this mechanism, the alkene dioxygenation is primarily determined by the reaction between the alkene and $^{\bullet}CO_3^-$ (step 2). As shown in Fig. S20a (ESI†), the conversion rate of various *para*-substituent α-methyl-styrenes exhibit well linear relationships with the Hammett constants of the substituents, with a negative slope ($\rho = -0.56$). The negative linear free energy relationship verifies that the rate-determining step for the oxidation of alkenes involves electrophilic attack by $^{\bullet}CO_3^-$. However, as shown in Table 2, relatively lower yields were obtained for α-methyl-styrene with electron-donating groups (such as $-OCH_3$ (**6a**), $-CH_3$ (**7a**)). In contrast to the negative slope observed for the oxidation rate, there is a positive strong correlation between the selectivity for the diol and the Hammett constants of the substituents (Fig. S20b, ESI†), implying that the selectivity for the diol is determined by a nucleophilic process. According to our proposed mechanism, the reduction of peroxydiol to diol by $^{\bullet}CO_3^-$ involves the nucleophilic attack of the peroxy moiety of peroxydiol by $^{\bullet}CO_3^-$. The substitution of an electron-withdrawing group would decrease the electron density on the peroxy bond, thereby facilitating its cleavage during the nucleophilic attack of $^{\bullet}CO_3^-$. The positive correlation further confirms that the reduction of peroxydiol to diol by $^{\bullet}CO_3^-$ is the selectivity-determining step in the dioxygenation reaction.

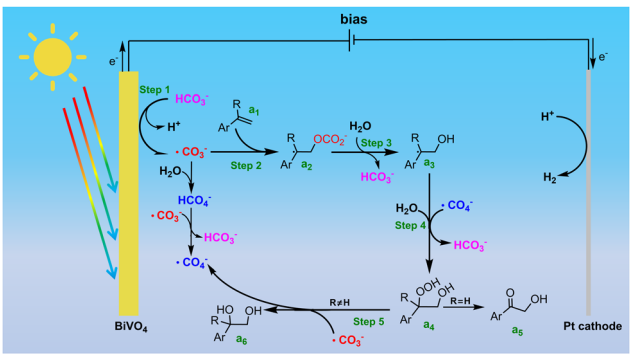

Scheme 2 The proposed HCO_3^--mediated dioxygenation mechanism on $BiVO_4$.

Conclusions

We developed a novel method for PEC bicarbonate-mediated alkene dioxygenation under mild conditions, coupled with the HER at the cathode, in which no noble metals or external oxidants are used. The PEC dioxygenation shows satisfying product selectivity and functional group tolerance, rendering the reaction straightforward, safe and amenable to diverse applications. Mechanistic studies verified the triple role played by HCO_3^--derived radicals: firstly, as initiators of alkene reactions through $^{\bullet}CO_3^-$; secondly, $^{\bullet}CO_4^-$ reacts with carbon radicals and undergoes further hydrolysis to form peroxyl alcohol intermediates; and thirdly, $^{\bullet}CO_3^-$ serves as a reductant to facilitate the transformation from peroxyl alcohols to a diol product. As a result, this innovative strategy provides a scalable, highly efficient and economically feasible route for synthesizing a diverse range of high added-value diols or α-hydroxy ketones derivatives.

Author contributions

J. Y. and C. C. conceived the idea. J. Y. designed and performed the experiments. J. Y., Y. K. Z. and M. D. analyzed the experiments data. J. Y., Y. F. Z. and J. L. analyzed the spin-trapped electron paramagnetic resonance (EPR) experiments. J. Y., C. C. and Y. L. analyzed the reaction mechanism. J. Y. and Y. K. Z. wrote the manuscript. Y. L. and C. D. helped with the writing. C. C., J. Z. and W. S. reviewed, edited the manuscript, and supervised the projects and processes. All authors have given approval to the final version of the manuscript.

Conflicts of interest

There are no conflicts to declare.

Acknowledgements

This work was supported by the National Natural Science Foundation of China (no. 22136005, 22188102, 22106164) and the Strategic Priority Research Program of Chinese Academy of Sciences (Grant No. XDB36000000).

References

1 H. G. Cha and K. S. Choi, *Nat. Chem.*, 2015, **7**, 328–333.
2 Y. Zhang, H. Zhang, A. Liu, C. Chen, W. Song and J. Zhao, *J. Am. Chem. Soc.*, 2018, **140**, 3264–3269.
3 S. Wang, G. Liu and L. Wang, *Chem. Rev.*, 2019, **119**, 5192–5247.
4 S. Chae, J. Choi, Y. Kim, D. L. T. Nguyen and O. Joo, *Angew. Chem., Int. Ed.*, 2019, **58**, 16395–16399.
5 Q. Zeng, J. Li, L. Li, J. Bai, L. Xia and B. Zhou, *Appl. Catal., B*, 2017, **217**, 21–29.
6 R. Song, H. Chi, Q. Ma, D. Li, X. Wang, W. Gao, H. Wang, X. Wang, Z. Li and C. Li, *J. Am. Chem. Soc.*, 2021, **143**, 13664–13674.
7 Z. Q. Wang, Y. H. Guo, M. Liu, X. L. Liu, H. P. Zhang, W. Y. Jiang, P. Wang, Z. K. Zheng, Y. N. Liu, H. F. Cheng, Y. Dai, Z. Y. Wang and B. B. Huang, *Adv. Mater.*, 2022, **34**, 27.
8 X. Liu, Z. Chen, S. X. Xu, G. Q. Liu, Y. Zhu, X. Q. Yu, L. C. Sun and F. Li, *J. Am. Chem. Soc.*, 2022, **144**, 19770–19777.
9 P. Rajeshwaran, J. Trouve, K. Youssef and R. Gramage-Doria, *Angew. Chem., Int. Ed.*, 2022, **61**, 50.
10 P. Xie, C. Xue, J. F. Luo, S. S. Shi and D. D. Du, *Green Chem.*, 2021, **23**, 5936–5943.
11 B. de Bruin, P. H. M. Budzelaar and A. W. Gal, *Angew. Chem., Int. Ed.*, 2004, **43**, 4142–4157.
12 Y. Zhao, M. Duan, C. Deng, J. Yang, S. Yang, Y. Zhang, H. Sheng, Y. Li, C. Chen and J. Zhao, *Nat. Commun.*, 2023, **14**, 1943.
13 W. R. Leow, Y. Lum, A. Ozden, Y. H. Wang, D. H. Nam, B. Chen, J. Wicks, T. T. Zhuang, F. W. Li, D. Sinton and E. H. Sargent, *Science*, 2020, **368**, 1228.
14 M. J. Chung, K. Jin, J. S. Zeng and K. Manthiram, *ACS Catal.*, 2020, **10**, 14015–14023.
15 K. Fuku and K. Sayama, *Chem. Commun.*, 2016, **52**, 5406–5409.
16 X. J. Shi, S. Siahrostami, G. L. Li, Y. R. Zhang, P. Chakthranont, F. Studt, T. F. Jaramillo, X. L. Zheng and J. K. Norskov, *Nat. Commun.*, 2017, **8**, 701.
17 T. M. Gill, L. Vallez and X. Zheng, *ACS Energy Lett.*, 2021, **6**, 2854–2862.
18 L. Fan, X. W. Bai, C. Xia, X. Zhang, X. H. Zhao, Y. Xia, Z. Y. Wu, Y. Y. Lu, Y. Y. Liu and H. T. Wang, *Nat. Commun.*, 2022, **13**, 2668.
19 F. Y. Chen, L. G. Xia, Y. Zhang, J. Bai, J. C. Wang, J. H. Li, M. Rahim, Q. J. Xu, X. Y. Zhu and B. X. Zhou, *Appl. Catal., B*, 2019, **259**, 118071.
20 L. G. Xia, F. Y. Chen, J. H. Li, S. Chen, J. Bai, T. S. Zhou, L. S. Li, Q. J. Xu and B. X. Zhou, *J. Hazard. Mater.*, 2020, **389**, 122140.
21 F. Boccini, A. S. Domazou and S. Herold, *J. Phys. Chem. A*, 2004, **108**, 5800–5805.
22 J. E. Grebel, J. J. Pignatello and W. A. Mitch, *Environ. Sci. Technol.*, 2010, **44**, 6822–6828.
23 C. P. Park, J. H. Lee, K. S. Yoo and K. W. Jung, *Org. Lett.*, 2010, **12**, 2450–2452.
24 C. M. Ho, W. Y. Yu and C. M. Che, *Angew. Chem., Int. Ed.*, 2004, **43**, 3303–3307.
25 X. H. Huo, R. He, X. Zhang and W. B. Zhang, *J. Am. Chem. Soc.*, 2016, **138**, 11093–11096.
26 B. M. Trost and L. R. Terrell, *J. Am. Chem. Soc.*, 2003, **125**, 338–339.
27 E. N. Jacobsen, I. Marko, W. S. Mungall, G. Schroder and K. B. Sharpless, *J. Am. Chem. Soc.*, 1988, **110**, 1968–1970.
28 S.-N. Chen, M. Z. Hoffman and G. H. Parsons, Jr, *J. Phys. Chem. C*, 1975, **79**, 1911–1912.
29 T. Zeng and W. A. Arnold, *Environ. Sci. Technol.*, 2013, **47**, 6735–6745.
30 P. Lianos, *Appl. Catal., B*, 2017, **210**, 235–254.
31 C.-Y. Huang, J. Li and C.-J. Li, *Nat. Commun.*, 2021, **12**, 4010.
32 A. K. Seitz, P. J. Kohlpaintner, T. Lingen, M. Dyga, F. Sprang, M. Zirbes, S. R. Waldvogel and L. J. Goossen, *Angew. Chem., Int. Ed.*, 2022, **61**, 25.
33 J. Liu, Y. Zou, B. Jin, K. Zhang and J. H. Park, *ACS Energy Lett.*, 2019, **4**, 3018–3027.
34 X. J. Yang, Y. H. Duan, J. L. Wang, H. L. Wang, H. L. Liu and D. L. Sedlak, *Environ. Sci. Technol. Lett.*, 2019, **6**, 781–786.
35 L. Chen, S. Wang, Z. Yang, J. Qian and B. Pan, *Appl. Catal., B*, 2021, **292**, 120193.
36 X. Sun, X. Li, S. Song, Y. Zhu, Y. F. Liang and N. Jiao, *J. Am. Chem. Soc.*, 2015, **46**, 6059–6066.
37 B. Yang and Z. Lu, *Chem. Commun.*, 2017, **53**, 12634–12637.
38 D. E. Richardson, H. R. Yao, K. M. Frank and D. A. Bennett, *J. Am. Chem. Soc.*, 2000, **122**, 1729–1739.
39 K. S. Haygarth, T. W. Marin, I. Janik, K. Kanjana, C. M. Stanisky and D. M. Bartels, *J. Phys. Chem. A*, 2010, **114**, 2142–2150.